JOURNAL OF MATERIALS SCIENCE **35** (2000) 4607–4613

Formation of the $La_{0.03}Sr_{0.255}Ba_{0.7}Nb_{2-y}Ti_yO_{6-y/2}$ ferroelectric ceramic system

H. AMORÍN, J. PORTELLES
Facultad de Física-Instituto de Materiales y Reactivos, Universidad de la Habana, San Lázaro y L, Vedado, La Habana 10400, Cuba; Centro de Ciencias de la Materia Condensada, UNAM, Apartado Postal 2881, Ensenada, 22800 B.C., Mexico

F. GUERRERO
Facultad de Ciencias Naturales, Universidad de Oriente, Santiago de Cuba 90500, Cuba

A. FUNDORA
Facultad de Física-Instituto de Materiales y Reactivos, Universidad de la Habana, San Lázaro y L, Vedado, La Habana 10400, Cuba; Centro de Ciencias de la Materia Condensada, UNAM, Apartado Postal 2881, Ensenada, 22800 B.C., Mexico

E. MARTÍNEZ, J. M. SIQUEIROS
Centro de Ciencias de la Materia Condensada, UNAM, Apartado Postal 2881, Ensenada, 22800 B.C., Mexico
E-mail: jesus@ccmc.unam.mx

The study of the formation of the $Sr_{0.255}La_{0.03}Ba_{0.7}Nb_{2-y}Ti_yO_{6-y/2}$ ferroelectric ceramic system and the influence of the sintering conditions and titanium concentration on the densification process is reported. A single-phase compound is observed for low titanium content ($y \leq 0.1$) in the XRD spectra, being isostructural with the tetragonal tungsten bronze SBN phase. For high titanium concentrations ($y > 0.1$) the XRD patterns show, besides the tetragonal phase reflections, several small peaks evidencing an additional phase in the compound. This second phase was identified as isostructural to hexagonal $Ba_6Nb_9Ti_7O_{42}$. The grain size shows a linear increase with titanium content in the region of monophasic compositions and a possible liquid phase aided sintering process is analyzed. © *2000 Kluwer Academic Publishers*

1. Introduction

Strontium-Barium Niobate (SBN) solid solutions have proved to be very useful in many applications such as pyroelectric detectors [1, 2], photorefractive materials [3] and electro-optic [4] and surface acoustic wave (SAW) [5] devices. Since the production of materials in single crystal form is usually very expensive [6], the design and production of ferroelectric ceramics [7] and, in particular SBN [8–10], has drawn increasing interest. The ease of fabrication, chemical and mechanical stability and the possibility of optimization of their properties by ion substitution in their crystalline structure, are some of the advantages of polycrystalline ceramics [11, 12].

Many investigations on the dielectric properties of ferroelectric ceramics such as permittivity, pyroelectricity and aging have shown them to be strongly dependent on the fabrication process [9, 12]. Even though the properties of the ceramics are often similar to those of single crystal materials [8, 9], their behavior is strongly conditioned by the grain morphology and grain boundaries, which contribute additional effects that must be considered [13]. The selection process of the sintering parameters that will produce the ceramic with the best properties becomes very important [14, 15]. The modification of the SBN system by rare earth and/or other elements strongly affects the material properties, including their transition temperature [16, 17]. In particular, the dielectric and pyroelectric properties can be optimized for room temperature applications [17, 18]. On the other hand, the addition of specific impurities in certain ferroelectric ceramics may produce the conditions that favor a fast densification process [14, 15]. In previous work, the influence of small amounts of lanthanum in the sintering of SBN based ceramics has been reported [11, 19]. Here, the effect of titanium content on the formation process of the $Sr_{0.255}La_{0.03}Ba_{0.7}Nb_{2-y}Ti_yO_{6-y/2}$ (LSBNT) ceramic system is presented.

2. Experimental procedure

High purity grade (>99.9%) $BaCO_3$, $SrCO_3$, La_2O_3, Nb_2O_5 and TiO_2 raw materials were used for the preparation of $Sr_{0.255}La_{0.03}Ba_{0.7}Nb_{2-y}Ti_yO_{6-y/2}$ samples, where y is 0.01 (LSBNT1), 0.03 (LSBNT3), 0.05

(LSBNT5), 0.1 (LSBNT10), 0.2 (LSBNT20) and 0.5 (LSBNT50), trough the conventional ceramic technique. The powders were mixed in an agate mortar with ethyl alcohol for 2 hours and calcined at 1100° C for 2 hours. The resulting powders were uniaxially die-pressed at 612 Mpa into discs of 10 mm diameter and 1 mm thickness, and sintered for several temperatures in air for 1 and 5 hours.

The density of the sintered samples was calculated by directly measuring their volume and weight them. The sintered samples were examined by X-ray diffraction (XRD) using Cu K_α radiation and a 0.02 °/step. The analysis of the obtained reflections by means of the PC-APD software and the 1997 PDF Database [20], allowed us to identify the crystalline phases present in the samples. The microstructure was observed using a Jeol JSM-5300 Scanning Electron Microscope (SEM) and the mean grain size was determined by the line intersection method [14].

3. Results and discussion

Fig. 1 shows the XRD patterns for samples with different compositions sintered at 1250° C for 5 hours. All the reflection peaks on the XRD patterns of the LSBNT1 and LSBNT10 samples coincide with those reported in the literature for SBN, that is, a tetragonal tungsten bronze (TTB) structure [21]. Similar patterns were obtained for intermediate compositions, indicating that for low titanium content monophasic compounds, isostructural with SBN, were produced.

In the LSBNT20 sample, beside the reflections corresponding to the TTB system, several small peaks appear evidencing an additional phase in the compound. Such additional peaks are better defined in the XRD patterns of the LSBNT50 sample (see Fig. 1). The increment of the titanium content in the compound results in an enhancement in the intensity of the peaks of the additional phase. This second phase was identified as isostructural to the hexagonal $Ba_6Nb_9Ti_7O_{42}$ (BNT) reported in the 1997 PDF Database [20]. This result suggests the existence of a solubility limit in the substitution of niobium by titanium in the TTB structure of the LSBN system, producing a polyphasic material for titanium concentrations above $y = 0.1$, as can be seen in the XRD patterns.

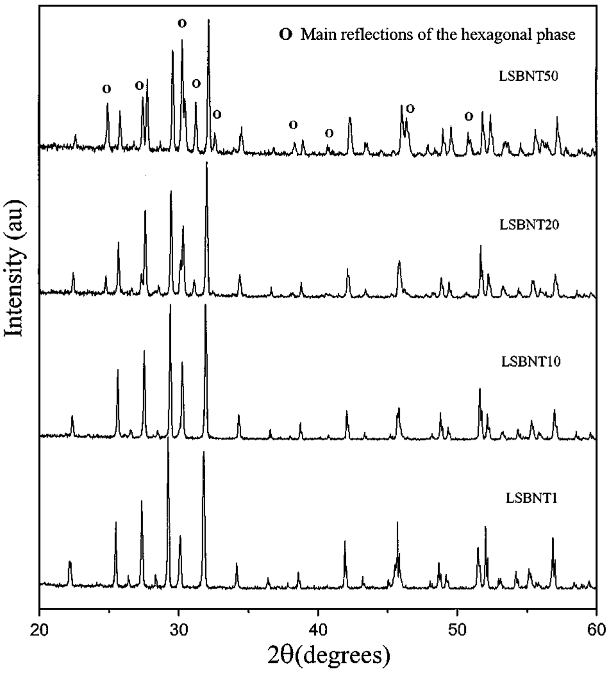

Figure 1 XRD patterns for $Sr_{0.255}La_{0.03}Ba_{0.7}Nb_{2-y}Ti_yO_{6-y/2}$ ceramics with different titanium content, sintered at 1250° C for 5 hours. The peaks corresponding to the hexagonal phase isostructural to $Ba_6Nb_9Ti_7O_{42}$ are indicated.

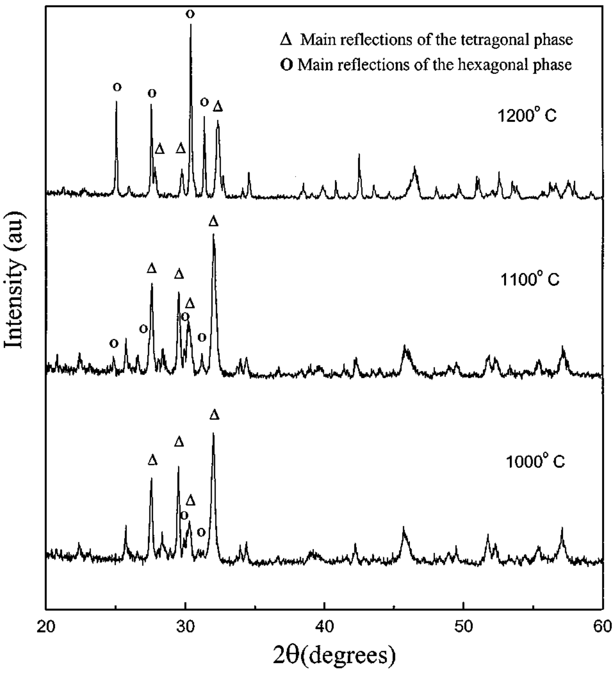

Figure 2 XRD patterns for the $Sr_{0.255}La_{0.03}Ba_{0.7}Nb_1Ti_1O_{5.5}$ sample calcined at different temperatures for 2 hours.

In accordance to the kinetics of crystallization of the $Sr_{0.255}La_{0.03}Ba_{0.7}Nb_1Ti_1O_{5.5}$ system as a function of firing temperature shown in Fig. 2, where equal molar amounts of titanium and niobium are used, the second phase seems to be generated from the TTB structure as the material is being processed. In this graphical sequence, it is seen how the TTB phase develops initially at a temperature of 1000° C, with the peaks associated to the hexagonal phase being very small, and without the presence of the intermediate compounds of the SBN phase ($BaNb_2O_6$ and $SrNb_2O_6$) in the XRD spectrum. For higher firing temperatures the hexagonal phase peaks start growing, while the TTB phase peaks become smaller as the temperature is increased. Finally, the hexagonal phase fully develops at 1200° C. All this facts suggest that the hexagonal phase grows at the expense of the TTB phase and not through intermediate compounds during the firing process.

The microstructure of the samples sintered at temperatures lower than 1250° C shows a high density of interconnected pores indicative of an early stage in the sintering process, as can be seen in Fig. 3a for the LSBNT1 sample sintered at 1200° C for 1 hour. The grain size is around 1 μm in all cases and a slight decrease in the porosity is observed with the increase in titanium concentration. Fig. 3b–e shows the microstructure of the LSBNT1, LSBNT5, LSBNT10

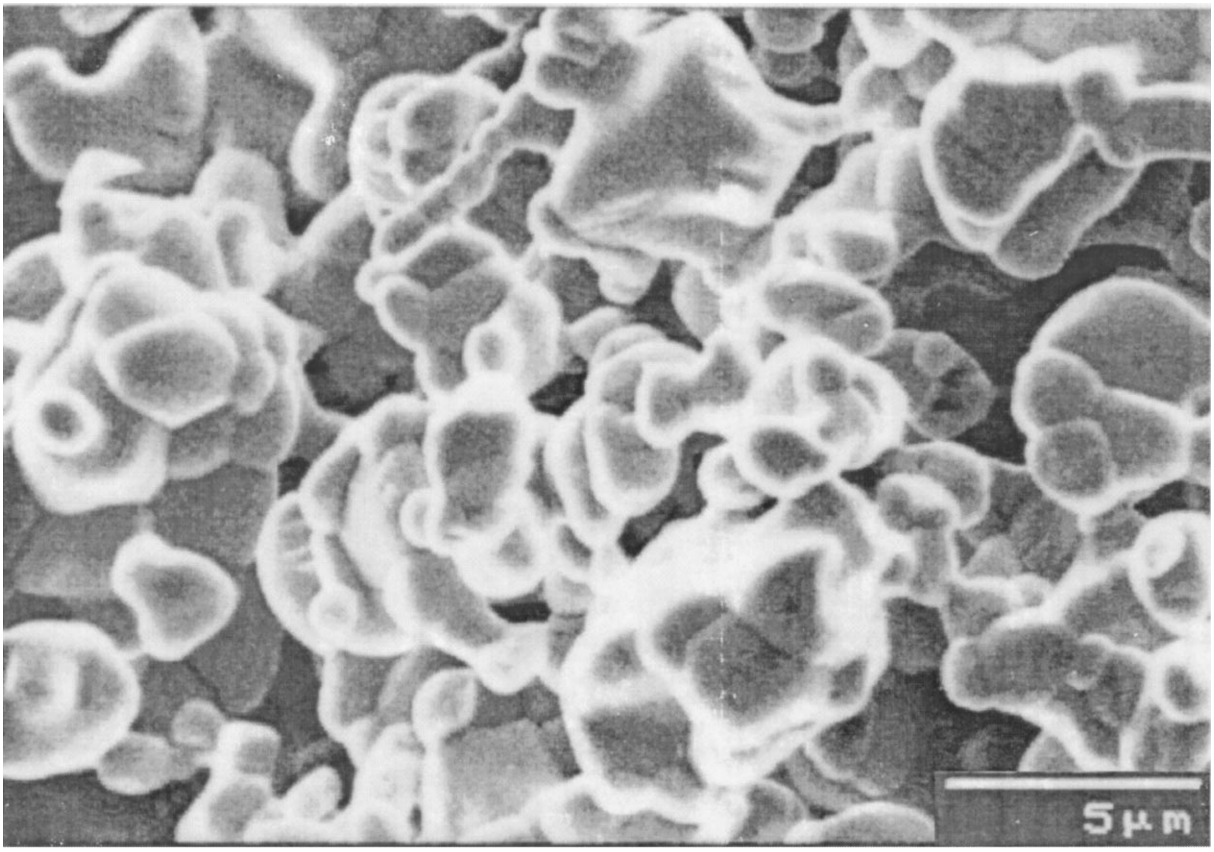

(a)

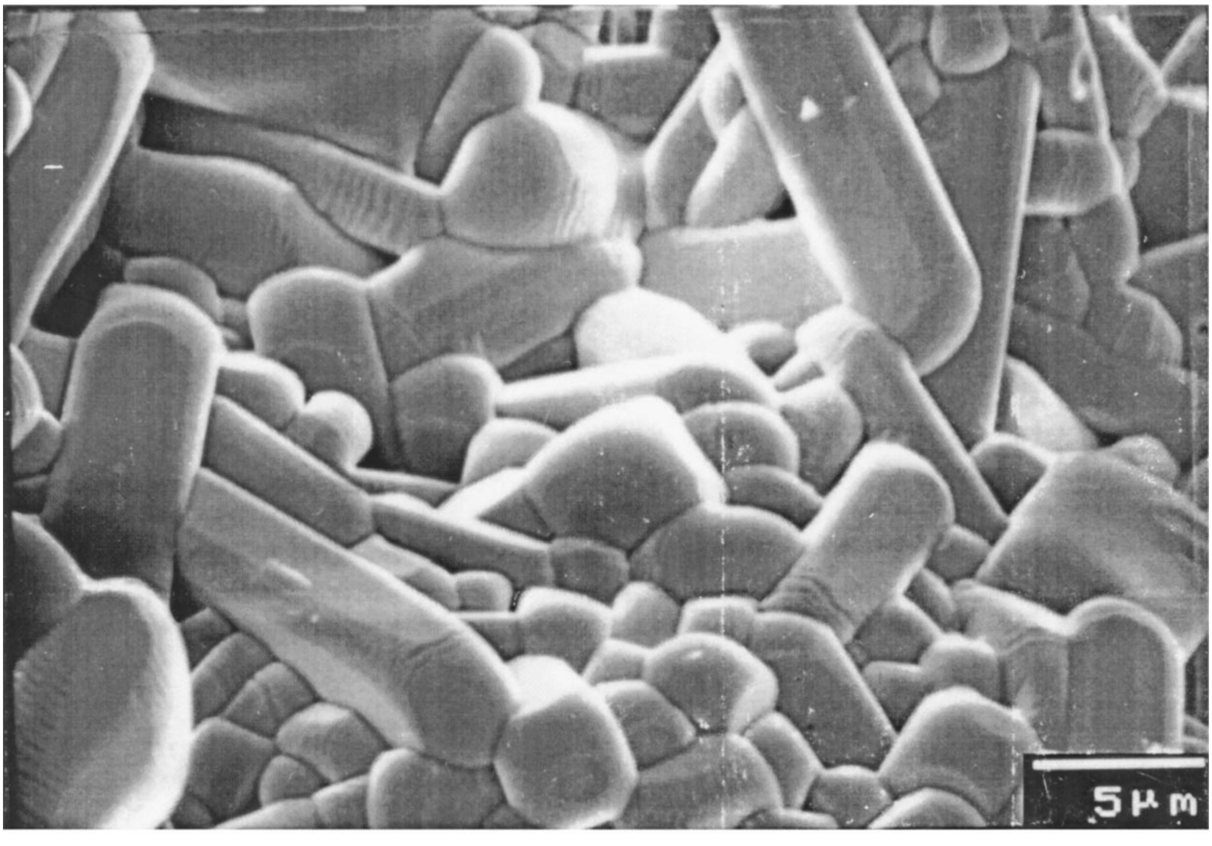

(b)

Figure 3 Microstructure of the (a) LSBNT1 sample sintered at 1200° C for 1 hour, and (b) LSBNT1, (c) LSBNT5, (d) LSBNT10 and (e) LSBNT50 samples sintered at 1250° C for 5 hours.

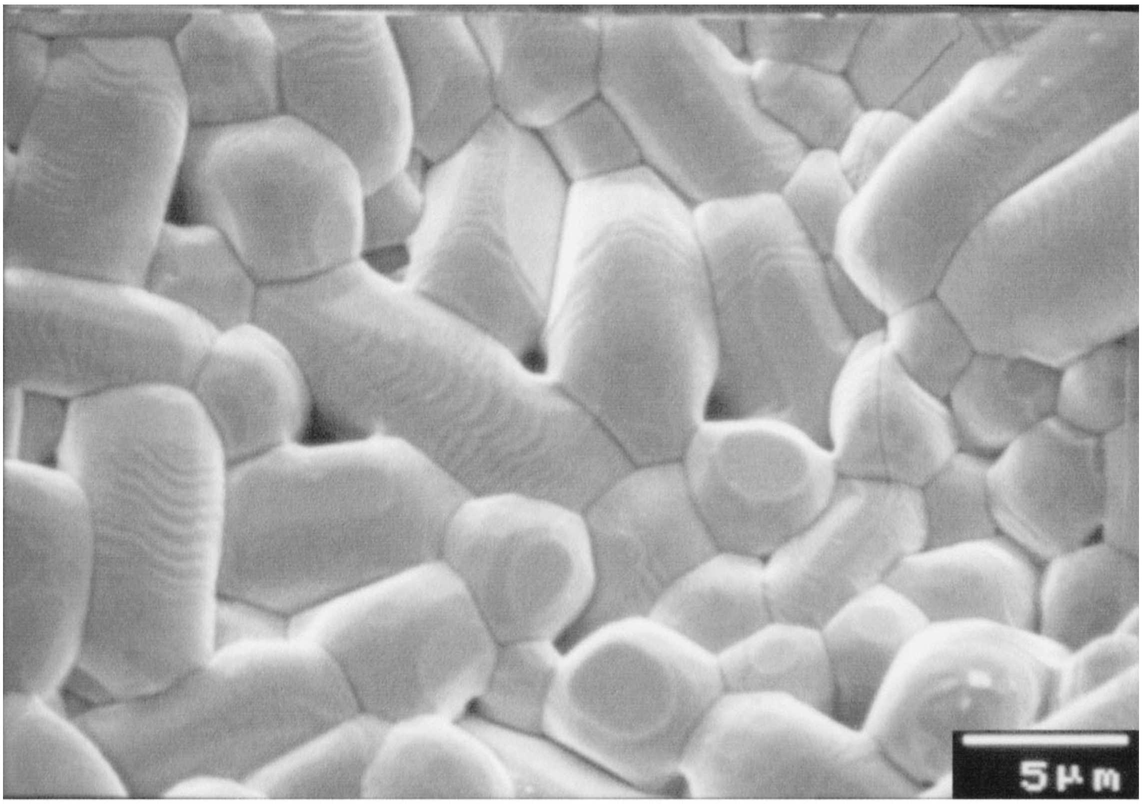

(c)

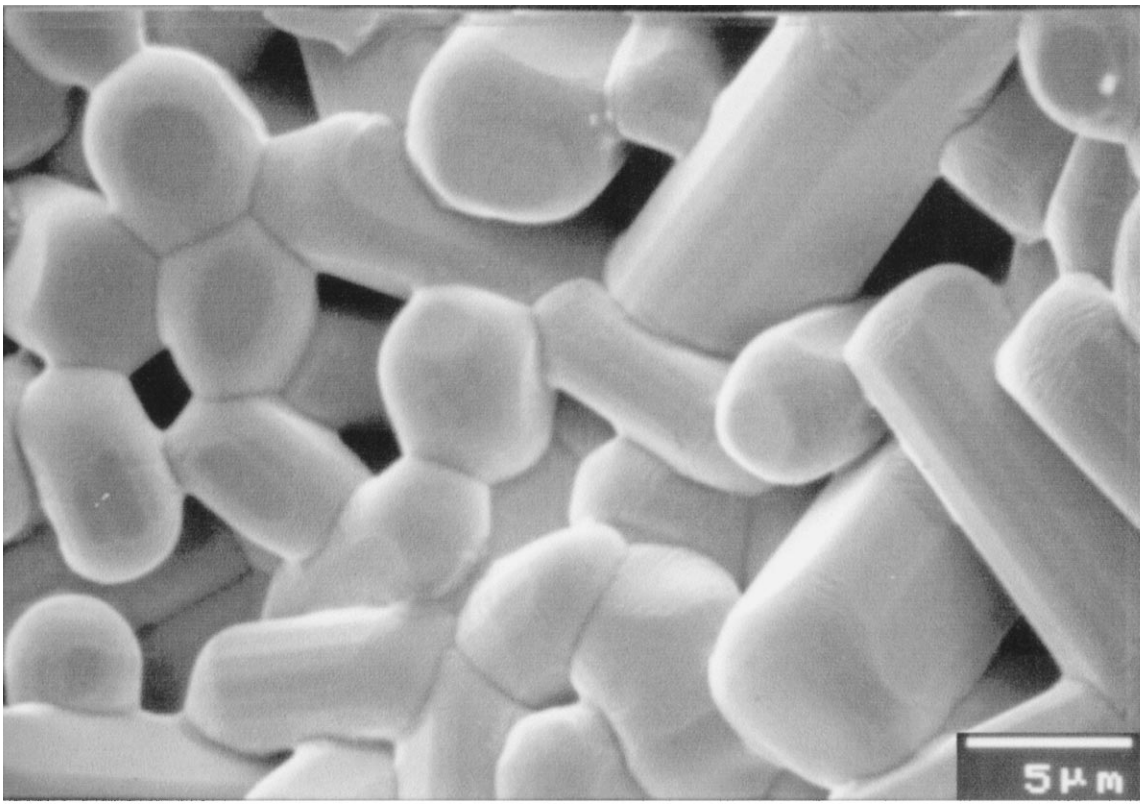

(d)

Figure 3 (*Continued*).

and LSBNT50 compositions, respectively, sintered at 1250° C for 5 hours. In all cases, compact ceramics with scarce non-interconnected porosity are observed, indicative of a late or final stage of the sintering process. Long bar-shaped grains predominate in the material. Similar microstructure was reported by Deshpande *et al.* [8] for SBN ceramics. The grain size shows a linear increase with titanium content in the region of monophasic compositions as can be seen in Fig. 4 while, for concentrations above $y = 0.1$ (polyphasic

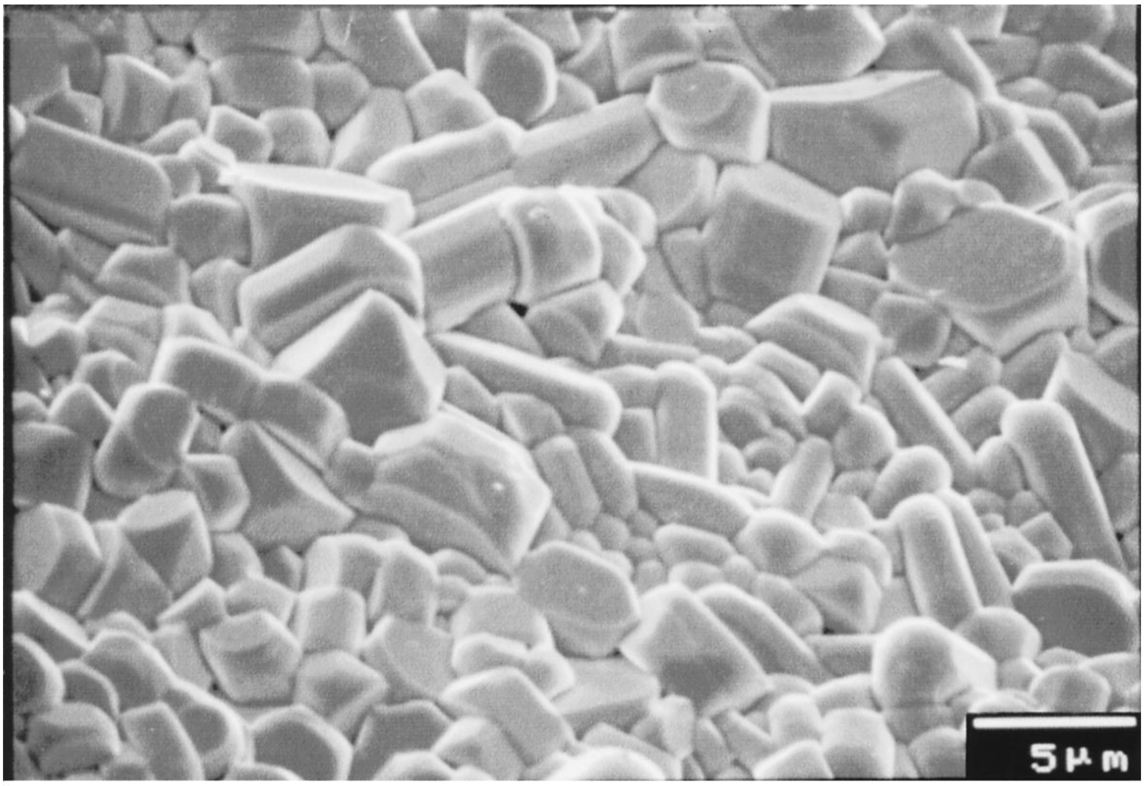

(e)

Figure 3 (*Continued*).

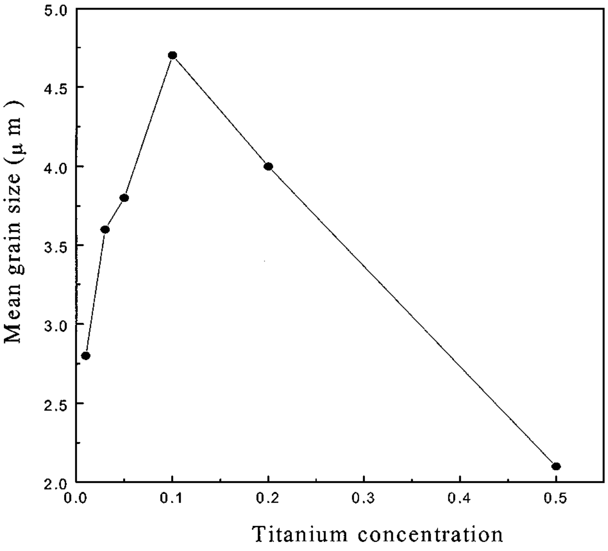

Figure 4 Grain size dependence with titanium content in samples sintered at 1250° C for 5 hours.

composition region) the grain size decreases, due possibly to the bimodal shape distribution of the grains shown in Fig. 3e for the LSBNT50 composition, with some long bar-shaped thin grains and large grains with regular form, possibly associated to the appearance of the hexagonal phase in the ceramic.

Grain growth in dense materials is associated to grain boundary motion. The driving force of this mechanism is the lowering of the boundary energy by the ion motion through the grain boundary [22]. These facts suggest that titanium substitution positively influence the sintering process in the monophasic compositions region by increasing the grain boundary motion and increasing the diffusion and densification kinetics that favor grain growth and the elimination of the porosity. For high titanium concentration the appearance of a hexagonal phase from the TTB phase forming a bimodal grain distribution microstructure influencing the grain growth and the densification process resulting in a lower average grain size.

Relative density curves plotted against sintering temperature for samples fired for 1 and 5 hours in the monophasic composition region are shown in Fig. 5a. For both sintering times, an increase in the relative density is observed from values around 75 and 85% in samples sintered at 1150° C for 1 and 5 hours, respectively, to values above 90% for samples sintered at 1250° C.

At higher sintering temperatures the density decreases for all compositions, that is, there is a maximum around 1250° C for the samples sintered for 1 hour and around 1200° C for samples sintered for 5 hours. It is worth mentioning in this respect, that the fabrication process of SBN or SBN based ceramics by the conventional ceramic technique requires energy consuming heat treatments at or above 1400° C [11]. However, for a sintering temperature of 1400° C a complete melting of the material was observed.

Fig. 5b shows the mass loss in the sintering process plotted against sintering temperature, where a sharp increase is observed for all compositions sintered above 1250° C, 5 hours. Under such sintering conditions, very rough materials were obtained and a flow of small amounts of liquid material was observed, producing stains in the oven bottom wall.

The presence of a liquid phase during the sintering process is suggested by the above mentioned facts, where two possibilities exist: (1) that an eutectic

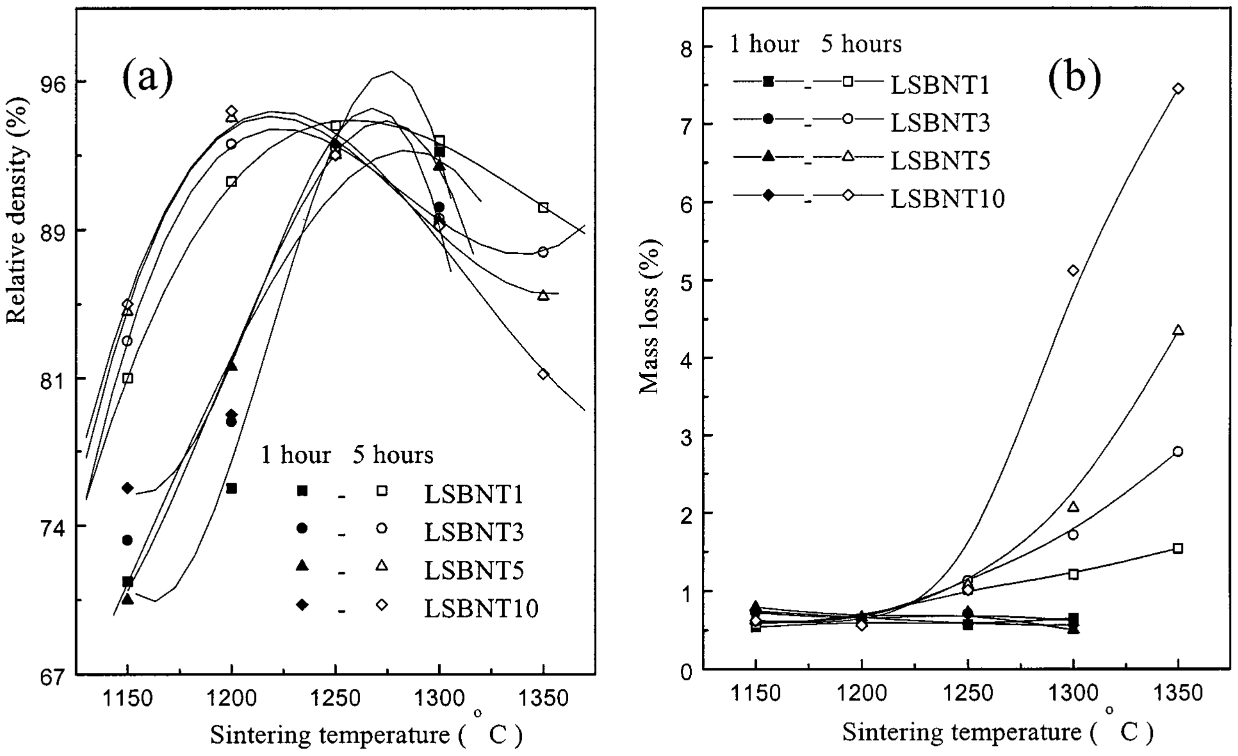

Figure 5 (a) Relative density curves and (b) mass loss in the sintering process plotted against sintering temperature for the $Sr_{0.255}La_{0.03}Ba_{0.7}Nb_{2-y}Ti_yO_{6-y/2}$ system fired for 1 and 5 hours, in the monophasic compositions region.

reaction takes place in the material in the presence of titanium that will have an associated liquid phase in the sintering process; or (2) a new phase with melting point around 1200° C is synthesized and takes part in the densification process.

XRD spectra showed no sign of additional phases for compositions below $y = 0.1$ of titanium, making more feasible the first possibility. Since the SBN system does not present any liquid phase or melting process within the used temperature interval [23], all the evidences suggest that such behavior be due to the addition of titanium to the ceramic system.

Sintering in the presence of liquid phase favors densification and mass transfer processes rendering better materials. This is a well-known fact reported in the literature, widely used to sinter materials that present difficulties in their densification process [15]. Densification processes in the presence of a liquid phase also favor, to a certain degree, the grain growth as the firing temperature approaches the melting temperature of the material that transforms to the liquid phase, where the mass transport process becomes very intense [14]. For higher temperatures, the density of the material may be reduced due to the loss of mass from the liquid phase and to trapped porosity that becomes thermodynamically stable and very hard to remove from the material. With the increase of titanium content, the mass loss becomes even higher reaching values between 4 and 7% for samples sintered at 1350° C.

For given values of the sintering temperature and time below that for maximum densification, the density of the samples will increase with titanium content, whether for temperatures above, the opposite will happen. Below the maximum density, higher titanium substitution favors the liquid phase formation and therefore, mass transport and densification. For temperatures above the maximum densification the liquid phase grows, destroying material with the consequent decrease of the density and the increase in mass loss. In samples with high titanium content ($y > 0.1$) a similar behavior was observed but the degradation and the melting of the samples occurred at lower temperatures.

A complete study on the ferroelectric properties of the system under study including P-E hysteresis measurements, pyroelectric behavior, ferroelectric to paraelectric phase transition, dependence of the transition temperature with Ti content, remanent polarization and other relevant properties have been reported in recently published papers [24, 25].

4. Conclusions

We have obtained the $Sr_{0.255}La_{0.03}Ba_{0.7}Nb_{2-y}Ti_y O_{6-y/2}$ ceramic system for different concentrations of titanium cation. A single phase compound is observed for low titanium content ($y < 0.1$) in the XRD spectra, being isostructural with the tetragonal tungsten bronze SBN phase. For high titanium concentrations ($y > 0.1$), the XRD patterns show, beside the tetragonal phase reflections, peaks associated with an additional phase present in the ceramics. This second phase was identified as isostructural to the hexagonal $Ba_6Nb_9Ti_7O_{42}$ and seems to be generated from the tetragonal structure as the material is being processed in the firing process. Such result suggests the existence of a solubility limit in the substitution of niobium by titanium in the tetragonal structure of the LSBN system. The grain size shows a linear increase with titanium content in the region of monophasic composition. The incorporation of titanium into the LSBN system leads to a liquid phase sintering with resulting relative densities above 90% of the theoretical value, possible due to an eutectic reaction in the material in the presence of titanium that would involve an associated liquid phase in the sintering process.

Acknowledgments

This work has been partially supported by CoNaCyT-México, through grant No. 26314E and by DGAPA-UNAM grant No. IN115098. We thank I. Gradilla and E. Aparicio for their technical support.

References

1. A. M. GLASS, *J. Appl. Phys.* **40**(12) (1969) 4699.
2. R. W. WHATMORE, P. C. OSBOND and N. M. SHORROCKS, *Ferroelectrics* **76** (1987) 351.
3. R. R. NEURGAONKAR and W. K. CORY, *J. Opt. Soc. Am. B: Opt. Phys.* **3**(2) (1986) 274.
4. P. V. LENZO, E. G. SPENCER and A. A. BALLMAN, *Appl. Phys. Lett.* **11**(1) (1967) 23.
5. R. R. NEURGAONKAR, M. H. KALISHER, T. C. LIM, E. J. STAPLES and K. L. KEESTER, *Mater. Res. Bull.* **15**(9) (1980) 1235.
6. K. MEGUMI, N. NAGATSUMA, Y. KASHIWADA, Y. FURUHATA, *J. Mater. Sci.* **11** (1976) 1583.
7. J. FERNÁNDEZ, P. DURAN and C. MOURE, *Bol. Soc. Esp. Ceram. Vidr.* **32**(1) (1993) 5.
8. S. DESHPANDE, H. POTDAR, P. GODBOLE and S. DATE, *J. Am. Ceram. Soc.* **75**(9) (1992) 2581.
9. N. VAN DAMME, A. SUTHERLAND, L. JONES, K. BRIDGER and S. WINZER, *ibid.* **74**(8) (1991) 1785.
10. S. NISHIWAKI, J. TAKAHASHI, K. KODAIRA and M. KISHI, *Jpn. J. Appl. Phys.* **35** (1996) 5137.
11. F. GUERRERO, J. PORTELLES, H. AMORÍN, A. FUNDORA, J. SIQUEIROS and G. HIRATA, *J. Europ. Ceram. Soc.* **18**(7) (1998) 745.
12. S. NISHIWAKI, J. TAKAHASHI and K. KODAIRA, *Jpn. J. Appl. Phys.* **33** (1994) 5477.
13. J.-C. M’PEKO, J. PORTELLES, F. CALDERON, G. RODRIGUEZ, *J. Mater. Sci.* **33** (1998) 1633.
14. M. A. AKBAS, M. A. McCOY and W. E. LEE, *J. Am. Ceram. Soc.* **78**(9) (1995) 2417.
15. J.-C. M’PEKO, J. PORTELLES and G. RODRÍGUEZ, *J. Mater. Sci. Lett.* **16** (1997) 1850.
16. F. GUERRERO, J. PORTELLES, I. GONZÁLEZ, A. FUNDORA, H. AMORÍN, J. SIQUEIROS and R. MACHORRO, *Solid State Comm.* **101**(6) (1997) 463.
17. S. T. LIU and R. B. MACIOLEK, *J. Electron. Mater.* **4**(1) (1975) 91.
18. H. AMORÍN, F. GUERRERO, J. PORTELLES, I. GONZÁLEZ, A. FUNDORA, J. SIQUEIROS and J. VALENZUELA, *Solid State Comm.* **106**(8) (1998) 555.
19. F. GUERRERO, H. AMORÍN, J. PORTELLES, J. SIQUEIROS and S. AGUILERA, *J. Electroceramics* **3**(4) (1999) 377.
20. JCPDS, International Center for Diffraction Data, 43-0962 (1997).
21. P. B. JAMIESON, S. C. ABRAHAMS and J. L. BERNSTEIN, *J. Chem. Phys.* **48**(11) (1968) 5048.
22. K. UMAKANTHAM, K. CHANDRAMOULI, G. NAGESWARA RAO and A. BHANUMATHI, *Bull. Mater. Sci.* **19**(2) (1996) 345.
23. M. E. LINES and A. M. GLASS, “Principles and Applications of Ferroelectric and Related Materials” (Clarendon Press, Oxford, 1977).
24. H. AMORÍN, J. PORTELLES, F. GUERRERO, J. PÉREZ, J. SIQUEIROS, *Solid State Communications* **113**(10) (2000) 581.
25. H. AMORÍN, J. PORTELLES, F. GUERRERO, A. FUNDORA and J. M. SIQUEIROS, *Journal of Electroceramics* **3**(4) (1999) 377.

Received 28 July 1999
and accepted 23 March 2000